

Bifurcation to chaos in the Bénard-Marangoni instability in a confined geometry.

S Rahal¹ and P Cerisier²

¹ Department of Mechanical Engineering, University of Batna, Rue Boukhlouf Mohamed el Hadi, 05000 Batna, ALGERIA.

² IUSTI - CNRS UMR 6595, Polytech'Marseille, Technopôle de Château-Gombert, 5 rue Enrico Fermi, 13453, Marseille Cedex 13, FRANCE.

Abstract: An experimental study of dynamical regimes in Bénard - Marangoni convection, for various Prandtl and Marangoni numbers, has been carried out in a confined geometry. Indeed, a small hexagonal vessel allowing the formation of only one convective cell, for a large extent of the Marangoni number, has been used. Fourier spectra and a correlation function have been used to recognize the various dynamical regimes. For fixed values of the Prandtl number and aspect ratio, an oscillatory, a quasi-periodic and chaotic states, were successively observed, as the Marangoni number was increased. The correlation dimensions of strange attractors corresponding to the chaotic regimes were calculated. The dimensions were found to be larger than those calculated by other authors for the Rayleigh-Bénard convection in small aspect ratio geometries. The transition from temporal chaos to spatio - temporal chaos has also been observed. Indeed for higher values of the Marangoni number, spatial dynamics are observed.

Key words: convection, Bénard, bifurcation, chaos, correlation dimensions.

1. Introduction:

In the hydrodynamical instabilities, chaotic dynamical regimes are often observed [1]. For example, in the convection instabilities, for a given convective pattern and a fixed value of the Rayleigh number, corresponds a dynamical regime. If the dynamics are chaotic, the observed chaos is temporal in a system for which spatial order is observed. Thus, temporal chaos is the name given to intrinsic randomness, i.e. random behaviour arising in a deterministic system. Temporal chaos in confined geometries has been observed in surface waves, Rayleigh-Bénard (RB) convection and in other hydrodynamical instabilities [1 – 3].

The case of small aspect ratios is interesting to examine because the confinement restricts the spectrum of modes allowed in extended geometries to few competing modes. Temporal and spatial modes can then be dissociated allowing thus the description of the dynamical behaviour of the system. Such study has been performed for RB instability. Indeed, many experiments have been performed on the transition to chaos in RB convection, including period doubling, intermittency, and quasi-periodicity [4]. Furthermore, measurements of the dimensions of attractors in RB chaotic regimes have confirmed the low dimensions at the onset of chaos in small aspect ratio systems [5], whereas the dimensions are larger for extended systems [6].

For Bénard-Marangoni (BM) convection (i.e., a horizontal fluid layer heated from below and cooled from above with an upper free surface), few works have been devoted to small vessels. These works dealt with the study of the onset of convection, the description of the convective patterns and the conditions of appearance of time-dependent flows [3]. More recently, a numerical study has been carried out on the transition to chaos for a fluid with a Pr number taken equal to zero [7].

The aim of this work is to recognize the different dynamical regimes which appear, when the vertical temperature difference is increased (Marangoni number increasing), using spectral methods and measuring the degree of strangeness of chaotic states by their correlation dimensions. As far as we know, such study has not been carried out. The convective spatial patterns were linked to the corresponding dynamical regimes by taking pictures of the structure. The influence of Marangoni and Prandtl numbers, and the aspect ratio, has been considered. The first results of this study are reported in this paper.

The outline of this paper is the following: experimental procedure and data analysis methods are described in section 2, typical experimental results are given in section 3; finally, some conclusions are given in section 4.

2. Experimental procedure and analysis methods:

2.1. Experimental set-up and procedure:

The use of the deflection of a laser beam by Bergé [4] allowed recognizing the various dynamical regimes and the transition to chaos in RB convection, for which the deflection is due only to the temperature gradients inside the liquid layer. In this work, a vertical laser beam has been used (Figure 1). The beam is reflected at first from the liquid-air interface (s) then the transmitted beam crosses the fluid layer perpendicularly to the horizontal (x, y) plane and is reflected from the bottom of the vessel (vs). The deflection (vs) is due to both the thermal gradients inside the fluid and the interface relief whereas the deflection (s) is due only to the interface deformation. On the screen (S), the deflections (s) and (vs) are recorded by a CCD camera and their values calculated thanks to software written by us. In this study only the beam (vs) has been considered. The time series recorded are then used to recognize and characterize the dynamical states using both spectral methods and dimensions of the attractors.

The dynamics described below take place in a hexagonal vessel (h) filled with silicon oil (F) (20 cst. or 50 cst. silicon oil) with lateral walls made of polycarbonate. The hexagonal vessel is surrounded by the same silicon oil which is limited laterally by the cylindrical container (C) (Figure 1). The fact that the polycarbonate has about the same thermal conductivity ($\lambda = 0.185 \text{ W/m}\times\text{K}$) as the silicone oil ($\lambda_1 = 0.16 \text{ W/m}\times\text{K}$) and owing to the existence of the oil guard ring, the lateral walls can be considered as thermally insulating.

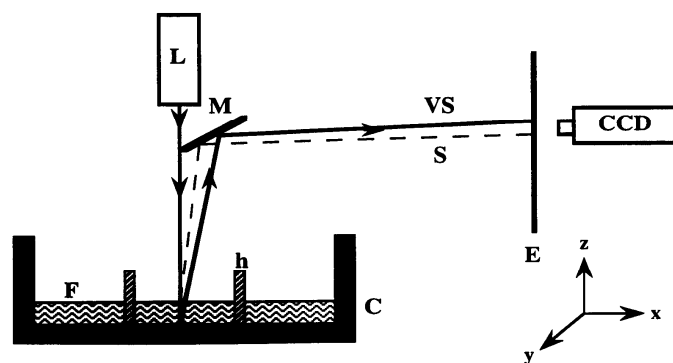


Figure 1. Experimental set-up. C: cylindrical container, h: hexagonal vessel, F: Fluid, M: Mirror, L: Laser, E: Screen, CCD: Camera.

The dynamical behaviour of the system depends on the spatial convective pattern [4]. Indeed, the relationship between the spatial patterns and the dynamical regimes, in small aspect ratios, has been studied in RB experiments. In order to link the dynamical regime to the corresponding spatial pattern, pictures of the pattern have been taken. The visualization has been achieved by seeding the silicon oil layer using aluminum flakes.

The dynamical behaviour of the system has been studied as a function of the Marangoni number (from 9.5 Ma to about 149 Ma , Ma is the critical value of Ma corresponding to the onset of convection), Prandtl number ($Pr_1 = 440$ for 50 cst. silicon oil, $Pr_2 = 160$ for 20 cst. silicon oil at 25°C) and the aspect ratio ($\Gamma_1 = 2.2$ ($d_1 = 1$ cm), $\Gamma_2 = 2.8$ ($d_2 = 0.8$ cm)), d being the depth of the silicon oil layer.

2.2. Analysis methods:

The distinction between periodical and chaotic regimes can be achieved using the power spectrum of the dynamical variable which is the laser beam deflection in our case. In a periodical regime (i.e., non-chaotic regime), the dynamical variable is a periodic or quasi-periodic function of time, therefore the power spectrum of the dynamical variable shows sharp peaks at the natural frequencies. On the other hand, in a temporally chaotic state, the power spectrum is continuous and does not show any sharp peaks.

As for the attractor, it may be a fixed point, a limiting cycle, or an n -torus; each of them involving a regular behaviour in the sense that the state of the system at any time can be deduced from its previous states. Alternatively, the regime may be irregular or chaotic. In this case, it is claimed that the motion takes place on a chaotic or strange attractor; the distance between two points in the phase space increasing exponentially with time. Indeed, infinitesimal uncertainties in the knowledge of the initial state of a temporally chaotic system are therefore magnified exponentially, and it is impossible to determine exactly the future state of the system.

The calculation method of the correlation dimension is as follows. Observation of a single variable $x(t)$ allows the estimation of the complete orbit in a phase space. The method used involves the reconstruction technique [8-10] which consists in the following: the motion on an attractor in a n -D phase space is parameterized by taking n displayed values of the variable, $x(t)$, $x(t + T)$, ..., $x(t + (n - 1)T)$; T being a delay time.

Strange attractors are typically characterized by a fractal correlation dimension (D) which is smaller than the number of degrees of freedom (F) of the system. The correlation dimension of an attractor is calculated from the locally measured time series by the method proposed by Grassberger and Procaccia [11, 12]. (D) is estimated by the exponent which is given by the asymptotic behaviour r^D of the integral correlation function $C(r, N)$:

$$C(r, N) = \frac{1}{N^2} \sum_{i, j=1 \neq j}^N H(r - |X_i - X_j|) \quad (1)$$

Where N is the total number of points, $H()$ is the Heaviside function and X_i is a vector in the n -D phase space obtained from the reconstructed time series using the delay time T . In practice, the correlation integral is evaluated by a sampling of reference points. The averaged number of points in hypersphers, centred on the reference points with radius r , was calculated to evaluate the above equation. The slope in the $\ln - \ln$ plot of $C(r)$, was determined using the least square method (Figure 2). $C(r)$ was evaluated using 18000 to 250000 data points in order to meet the *Tsonis* criterion which considers (N) required for reliable calculations of the correlation dimension (D) to be exponentially related to the correlation dimension (that is $N \sim 10^{2 + 0.4D}$), 100 reference points and a maximum dimension of the phase space equal to 16 were used.

The calculations have been carried out by increasing the dimension of the phase space until the convergence of the correlation dimension (D) is achieved. The software allowing the calculation of the

correlation dimension has been validated using periodical functions (mono periodical, $D = 1$ and bi-periodical, $D = 2$) and by calculating the dimensions of Hénon's model attractor ($D = 1.22$ with $N = 20000$, $a = 1.4$ and $b = 0.3$) and Coulet – Feigenbaum's model attractor ($D = 0.50$ with $N = 20000$, $\lambda = 3.57$). The dimensions, calculated using our software, are in good agreement with those calculated by other authors for the same theoretical model coefficients [13].

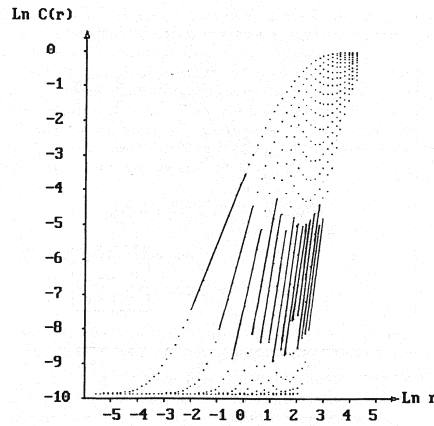


Figure 2. Integral correlation function for various dimensions (n) of the phase space ($\text{Ln} - \text{Ln}$ plot). (n) varies from 2 to 16 (from left to right), the slopes of linear regions give (D).

3. Typical results:

For the experiment carried out at $\text{Pr}_1 = 440$ and $\Gamma_1 = 2.2$, the first bifurcation observed above the onset of convection is analogous to the Hopf bifurcation in RB convection, which leads to a time - dependent regime. Indeed, for $\text{Ma} = 9.5 \text{ Mac}$, figure 3 shows a spectrum with one peak at the frequency $f_1 = 0.7 \text{ Hz}$ and its harmonics. By increasing Ma to 17 Mac , we observed a second peak at the frequency $f_2 = 1.1 \text{ Hz}$ (Figure 4). All the other peaks can be analyzed as linear combinations of the two fundamental frequencies.

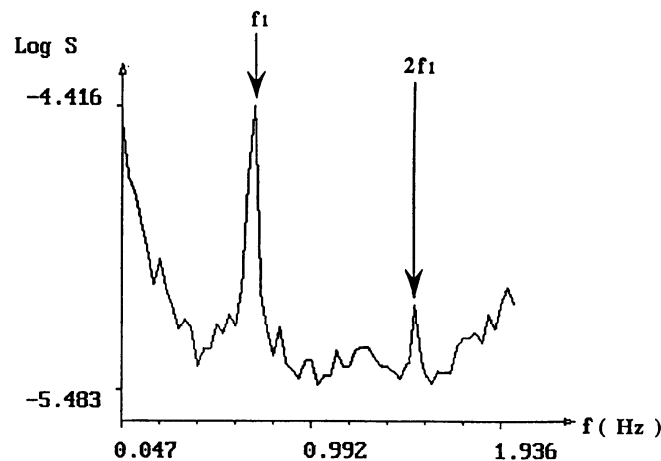


Figure 3. Fourier spectrum of the beam deflection. The fundamental frequency $f_1 = 0.7 \text{ Hz}$ and its harmonics. $\text{Ma} = 9.5 \text{ Mac}$; $\text{Pr}_1 = 440$ at $25 \text{ }^\circ\text{C}$; $\Gamma_1 = 2.2$.

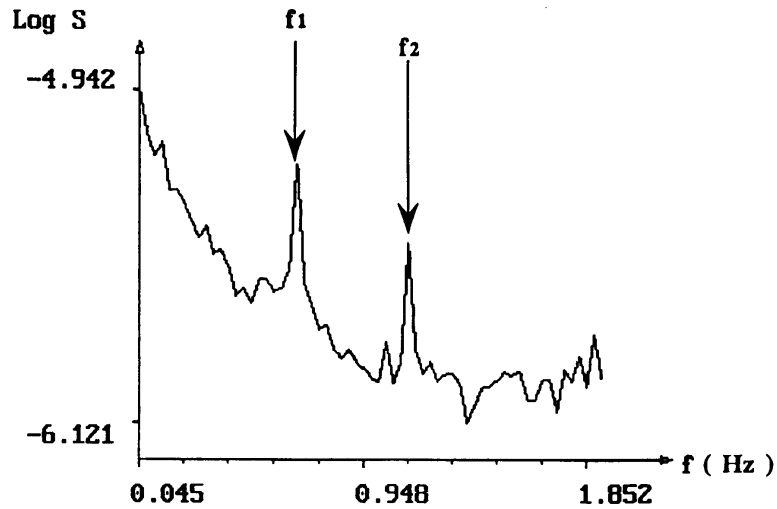


Figure 4. Fourier spectrum of the beam deflection. Bi-periodical regime. $Ma = 17 \text{ Mac}$; $Pr_1 = 440$ at $25 \text{ }^\circ\text{C}$; $\Gamma_1 = 2.2$; $f_1 = 0.7 \text{ Hz}$ and $f_2 = 1.1 \text{ Hz}$.

With a new increase of Ma to 25.5 Mac , we observe a chaotic state characterized by a spectrum which exhibits a broad band noise without any sharp peaks (figure 5) and a correlation function which vanishes for a long period of time (figure 6). A continuous spectrum and a correlation function which vanishes for a long period of time is an indication of the system memory loss, becoming thus unpredictable and consequently chaotic. Such transition to temporal chaos via the quasi-periodicity has been also observed in the RB instability [4].

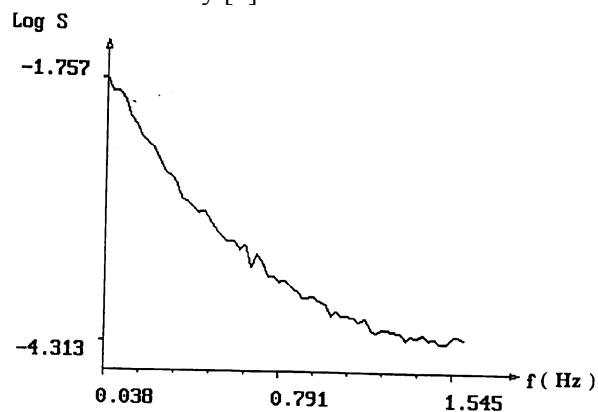


Figure 5. Fourier spectrum of the beam deflection. Chaotic regime. $Ma = 25.5 \text{ Mac}$; $Pr_1 = 440$ at $25 \text{ }^\circ\text{C}$; $\Gamma_1 = 2.2$.

The chaotic behaviour is also observed in figure 7 which shows three spectra corresponding to three values of Ma (65 Mac , 109 Mac and 149 Mac). As Ma is increased, the broad band noise spreads to higher frequencies. The appearance of a broad band in the frequency spectrum is the indication of the transition to a chaotic state. However, to know if this chaos is random or deterministic and to measure the degree of strangeness, these spectra cannot be used. The aim of attractor construction and correlation dimension calculation is to provide such information.

Thus, to follow quantitatively the evolution of the chaotic dynamical regimes with the increase of Ma , we have calculated the correlation dimensions of the corresponding attractors. It can be seen in figure 8 (a) that chaos develops as ΔT is increased and that (D) increases with decreasing Pr number.

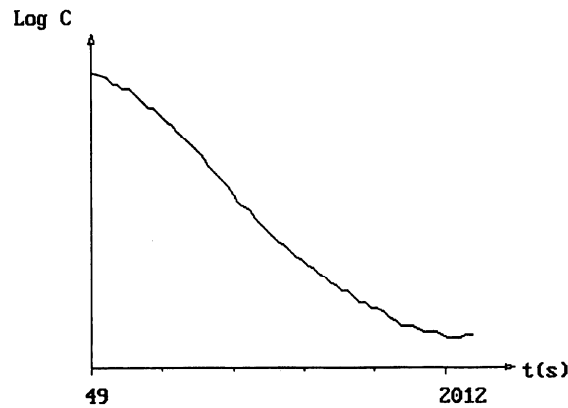


Figure 6. Auto - correlation of the beam deflection. Chaotic regime. $Ma = 25.5 \text{ Mac}$; $Pr_1 = 440$ at $25 \text{ }^\circ\text{C}$; $\Gamma_1 = 2.2$.

At $Pr_1 = 440$, the influence of the aspect ratio on the correlation dimension has been considered. The system is more complex for $\Gamma = 2.8$ than for a smaller aspect ratio ($\Gamma = 2.2$) (Figure 8(b)). This result has been also reached by Libchaber and Maurer [14], who showed for a RB experiment with helium, the large dependence of the temporal behaviour as a function of the aspect ratio. They observed periodical oscillations for $\Gamma < 3$ and chaotic regimes for $\Gamma > 3$.

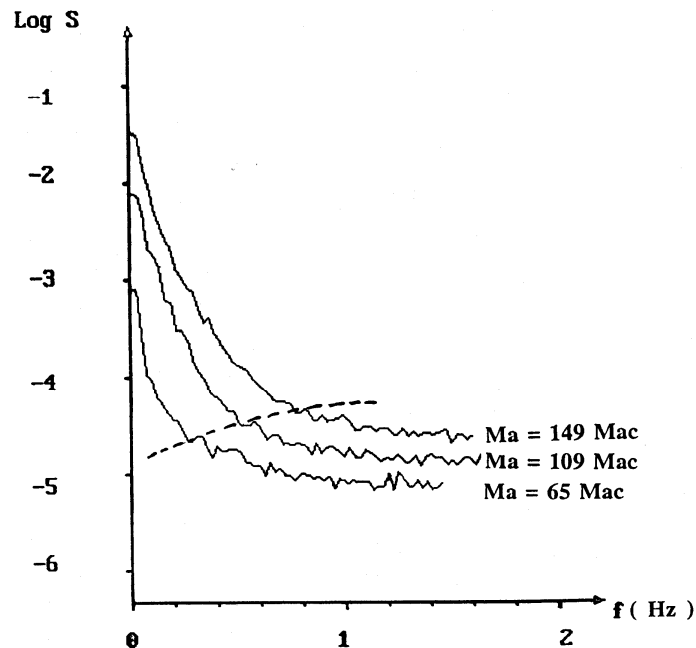


Figure 7. Fourier spectrum of the beam deflection. Chaotic regimes corresponding to various Ma . $Pr_1 = 440$ at $25 \text{ }^\circ\text{C}$; $\Gamma_1 = 2.2$.

As the dynamical regime is linked to the spatial convective pattern, pictures of the patterns have been taken. For example, Figure 9 shows pictures corresponding to the two values of the Pr number. Thus, one convective cell is observed for a large range of ΔT for $Pr_1 = 440$ than for $Pr_2 = 160$. A breaking of the convective cell is observed at $\Delta T = 10^\circ\text{C}$ for Pr_2 and at $\Delta T = 15 \text{ }^\circ\text{C}$ for Pr_1 . Thus for these values of ΔT , transitions to spatio-temporal chaos are observed with the mobility of the pattern and the involvement of the spatial modes.

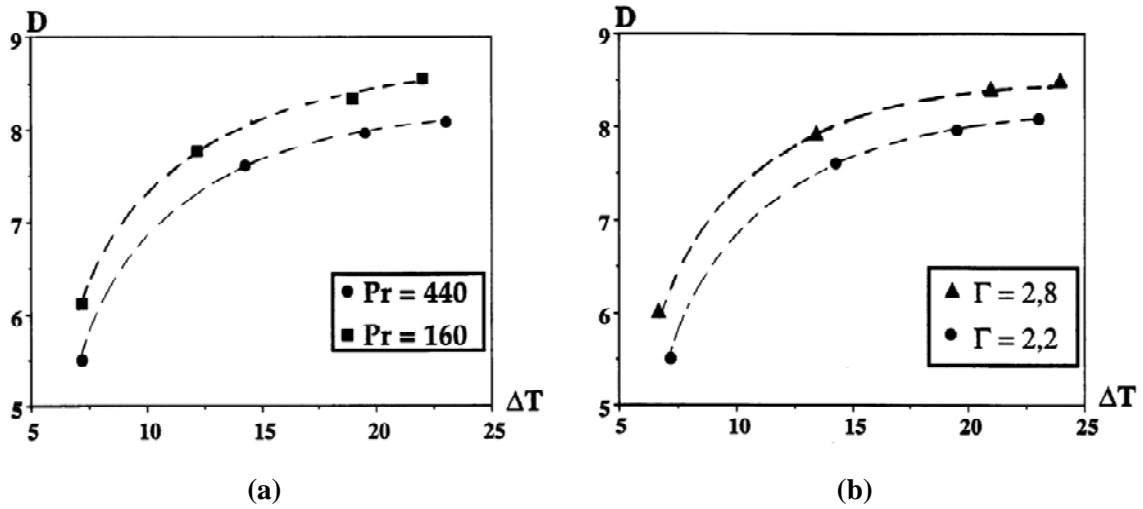


Figure 8. Variations of the correlation dimension as a function of ΔT , Pr and Γ .

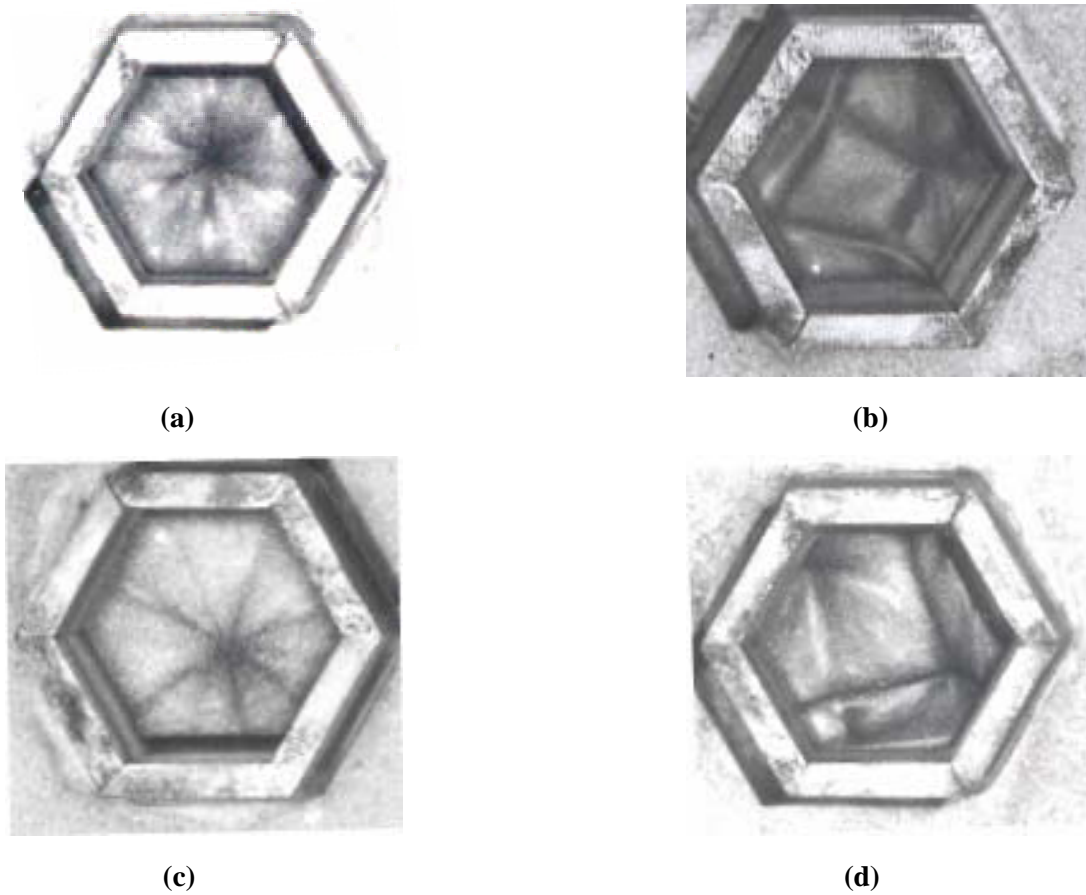


Figure 9. Pictures of the convective pattern, corresponding to various ΔT and Pr .
 $Pr_1 = 440$: (a) $\Delta T = 5^\circ C$; (b) $\Delta T = 19.5^\circ C$. Pr_2 : (c) $\Delta T = 5^\circ C$; (d) $\Delta T = 12.2^\circ C$.
 The structures in (b), (c) and (d) are moving, the shown patterns are observed for a given time.

4. Conclusions:

A transition to temporal chaos including the quasi-periodicity, as in RB convection, has been observed in BM convection in small aspect ratios ($\Gamma = 2.2$).

The calculated dimensions of attractors (about 5 to 9) for the BM instability are larger than those found for the RB instability in confined geometries [5] (2-3) but they are close to those found by Sato *et al.* [6] (6.5 or 9) in a quasi-one-dimensional RB system ($\Gamma_x = 15$ and $\Gamma_y = 1$). Indeed, in our experiment, in addition to convection in the liquid as in RB convection, both surface tension and convection in the air layer above the silicon oil are involved, so that the number of independent variables to specify is larger than in the RB instability in small aspect ratio geometries (the dimension of an attractor is linked to the number of independent variables to specify the state of the system at any given time).

The transition from temporal chaos to spatio-temporal chaos has also been observed. Indeed for higher values of the Marangoni number, spatial dynamics are observed.

References:

- [1] Cross M C and Hohenberg P E 1993 Pattern formation outside of equilibrium *Rev. Mod. Phys.* **65** 851 - 1112.
- [2] Bodenschatz E, Pesch W and Ahlers G 2000 Recent developments in Rayleigh-Bénard convection *Ann. Rev. Fluid Mech.* **32** 709 - 78.
- [3] Schatz M F and Neitzel G P 2001 Experiments on thermocapillary instabilities *Ann. Rev. Fluid Mech.* **33** (6) 93 - 127.
- [4] Bergé P 1988 *Le Chaos: théorie et expériences* (Eyrolles).
- [5] Dubois M and Bergé P 1986 Rotation number dependence at onset of chaos in free Rayleigh-Bénard convection *Physica Scripta* **33** 159 - 68.
- [6] Sato S, Sano M and Sawada Y 1988 Bifurcation to chaos and dimensionality of attractors in an extended Rayleigh-Bénard convection system *Phys. Rev. A* **37** 1679 - 83.
- [7] Boeck T, Vitanov N K 2002 Low dimensional chaos in zero Prandtl number Bénard-Marangoni convection *Phys Rev E* **65** 37203 - 6.
- [8] Takens F 1981 *Dynamical Systems and Turbulence* ed Rand D A and Young L S (Berlin: Springer - Verlag).
- [9] Takens F 1985 in *Dynamical Systems and Bifurcations* ed Broer H W and Takens F (New York: Springer - Verlag).
- [10] Packard N H, Crutchfield J P, Farmer J D and Shaw R S 1980 Geometry from a Time Series *Phys. Rev. Lett.* **45** 712 - 16.
- [11] Grassberger P and Procaccia I 1983 Characterization of Strange Attractors *Phys. Rev. Lett.* **50** 346 - 49.
- [12] Grassberger P and Procaccia I 1983 Measuring the strangeness of strange attractors *Physica D* **9** 189 - 208.
- [13] Lausberg C 1987, Ph. D thesis, INPG, Grenoble, France.
- [14] Libchaber A and Maurer J 1980 Une expérience de Rayleigh-Bénard en géométrie réduite; multiplication, accrochage et démultiplication de fréquences *Journal de Physique* **41C3** 51 - 56.